

SCIENTIFIC REPORTS



OPEN

Exciton-polariton Josephson junctions at finite temperatures

M. E. Lebedev¹, D. A. Dolinina¹, Kuo-Bin Hong², Tien-Chang Lu², A. V. Kavokin^{3,4,5} & A. P. Alodjants^{1,6}

We consider finite temperature effects in a non-standard Bose-Hubbard model for an exciton-polariton Josephson junction (JJ) that is characterised by complicated potential energy landscapes (PEL) consisting of sets of barriers and wells. We show that the transition between thermal activation (classical) and tunneling (quantum) regimes exhibits universal features of the first and second order phase transition (PT) depending on the PEL for two polariton condensates that might be described as transition from the thermal to the quantum annealing regime. In the presence of dissipation the relative phase of two condensates exhibits non-equilibrium PT from the quantum regime characterized by efficient tunneling of polaritons to the regime of permanent Josephson or Rabi oscillations, where the tunneling is suppressed, respectively. This analysis paves the way for the application of coupled polariton condensates for the realisation of a quantum annealing algorithm in presently experimentally accessible semiconductor microcavities possessing high (10^5 and more) Q-factors.

In the XXI century, the studies of exciton-polariton Bose-Einstein condensates (BEC) in various type of semiconductor microstructures have become an important area of research in photonics and semiconductor physics^{1,2}. Microcavity exciton polaritons are quasiparticles representing admixtures of quantized cavity photons and quantum well excitons. Semiconductor microcavities are promising for various optoelectronic applications where the quantum matter-field interface plays an essential role. In such systems low branch polaritons can be treated as a 2D weakly interacting bosonic gas.

The polariton lasers are currently available optoelectronic devices for which coherent emission (“lasing”) occurs due to BEC of low branch exciton-polaritons. Bosonic condensates of exciton-polaritons have been observed at elevated temperatures ranging from a few tens of Kelvin in GaAs and CdTe based microcavities to the room temperature in GaN, ZnO and organic microcavities. Polariton lasing is a spectacular example of the formation of a bosonic condensate of exciton-polaritons in a driven-dissipative system. Among the recent achievements of polaritonics it is worth to mention experimental demonstrations of polariton lasers with electrical injection^{3,4}, polariton amplifiers⁵, switches⁶, transistors⁷, polariton circuits and optical logic elements^{8,9}. Although exciton-polariton condensates exhibit the Bose-Einstein statistics above the lasing threshold and are characterized by a macroscopic occupation of the ground state at certain pumping rate that is less than the threshold pumping for convenient lasers, they are not in a true thermodynamic equilibrium state^{10,11}. Non-equilibrium features of exciton polariton condensates play an important role in various manifestations of their collective (many body) states such as superfluidity^{12,13}, quantized vortices^{14,15}, soliton formation¹⁶, Josephson oscillations and macroscopic self-trapping^{17,18}.

The problem of distinguishability of statistically classical (thermal) and quantum regimes for exciton-polariton condensates is very important in view of the possible exciton-polaritons applications in quantum information technologies¹⁹. Fast switching properties (the typical switching time of a few picoseconds), relatively strong non-linear response and flexibility to external optical and/or electrical pumping spin degrees of freedom made microcavity polaritons potentially promising for quantum computation and quantum information processing^{19–23}.

Here we specifically focus on the quantum annealing problem that is relevant to the searching algorithm for the global minimum of the potential energy landscape (PEL) consisting of a set of barriers and wells^{24,25}. In a purely classical (thermal) regime the bosonic quasiparticles cross barriers stochastically at finite temperature with

¹ITMO University, St. Petersburg, 197101, Russia. ²Department of Photonics, National Chiao Tung University, Hsinchu, 300, Taiwan. ³Spin Optics Laboratory, St. Petersburg State University, Ul’yanovskaya, Peterhof, St. Petersburg, 198504, Russia. ⁴School of Physics and Astronomy, University of Southampton, SO17 1BJ, Southampton, United Kingdom. ⁵Istituto CNR-SPIN, Viale del Politecnico 1, I-00133, Rome, Italy. ⁶Vladimir State University named after A. G. and N. G. Stoletovs, Gorkii Street 87, Vladimir, Russia. Correspondence and requests for materials should be addressed to A.P.A. (email: alexander_ap@list.ru)

Received: 20 April 2017

Accepted: 31 July 2017

Published online: 25 August 2017

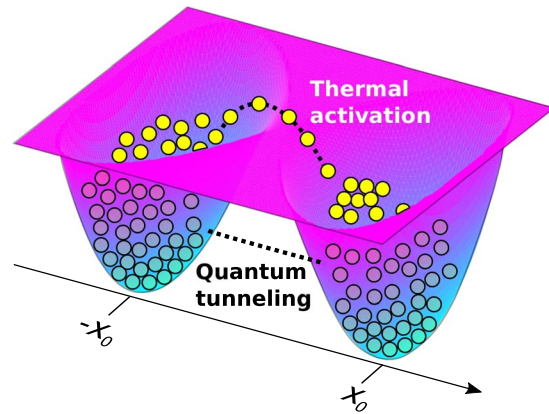


Figure 1. Sketch of two tunnel coupled exciton-polariton condensates. The two minima of the trapping potential U are situated at the points $+x_0$ and $-x_0$. At thermal equilibrium the interplay between thermal and quantum annealing effects is governed by the blue shift of condensates, effective temperature of exciton-polaritons and the shape of the potential.

the help of thermal activation process if the thermal energy is large enough, see Fig. 1. Contrary, in a quantum limit the same system undergoes quantum tunneling through the barrier. Obviously, the shape (height and thickness) of the barrier plays an essential role in this case^{25,26}. It has been shown recently in ref. 26 that the annealing algorithm relies in general case on the combination of thermal annealing and quantum tunneling. The collective (bosonic) character of polariton condensation could be used for the acceleration of the physical implementation of the search algorithm²⁷. The authors of refs 28, 29, propose polariton graphs as an analog platform for minimizing the XY-Hamiltonian by exploring the non-equilibrium character of exciton-polariton condensates and mimicking various magnetic phases with them. An original technique of nonresonant spatially modulated pumping beam have been used to imprint two-dimensional polariton graphs with different topology and different heights of potential barriers. Importantly, the phase-locking between arbitrary neighboring vertices might be practically achieved in this case.

In the present paper we study the effect of a finite effective temperature on the coupling of quasi-equilibrium exciton-polariton condensates accounting for the competing thermal and quantum annealing effects. To be more specific, here we examine an exciton-polariton Josephson junction (JJ) as a toy model for the classical or quantum annealing problem.

The Josephson effect initially discovered in superconductors³⁰ then has been studied in weakly coupled atomic BECs^{31–35}. Since the temperature of atomic Bose-Einstein condensation is extremely low (μK 's and below) it is usually possible to consider dynamical effects occurring with two atomic condensates confined in a W-shape potential using the mean field approach in zero temperature approximation. Josephson and Rabi oscillations, self-trapping of atoms and the population imbalance between potential traps have been reported^{36,37}.

JJ of exciton-polariton condensates is a relatively young Josephson coupled system that is being studied in many experimental laboratories around the Globe^{17,18,38–43}. It is important to underline that the polariton system is strongly different from superconducting and atomic JJs for several reasons, namely:

- (i) In superconducting JJ the tunnelling of electrically charged Cooper pairs is at the origin of coupling, while in the case of exciton-polariton condensates, electrically neutral exciton-polaritons tunnel.
- (ii) The mechanisms of dissipation are dramatically different in the systems. While Cooper pairs (or atomic BECs) are stable below critical temperature, exciton-polaritons are characterised by a radiative life-time: the features of the junctions essentially depend on the Q-factor of the cavity, which is why the exciton-polariton system needs to be considered as a driven-dissipative system by its origin
- (iii) All the most essential parameters of exciton-polariton JJ and superconductor/atomic systems: masses, characteristic length- and time-scales are dramatically different, see refs 12, 40–42.

Recently Yongbao Sun *et al.* reported⁴⁴ the observation of a quasi-equilibrium low branch exciton polariton condensate in a high Q-factor microcavity characterised by a remarkably long photon lifetime of 135 ps. Clearly, exciton-polaritons with long lifetime are promising candidates especially for quantum technologies²⁰.

One of the advantages of exciton-polaritons over cold atoms consists in a perspective of room temperature operation of polariton devices. In this context, it is very important to reveal the impact of temperature on the physics of interacting polariton condensates. It should be also noted that the effective temperature of a polariton gas may be introduced in the quasi-equilibrium approximation, which is not necessarily valid in all cases but constitutes an important starting point of any analysis. Further steps would involve a full kinetic modeling for a non-equilibrium polariton gas. We study the interplay of two mechanisms of coupling between the condensates in order to reveal the cross-over from the quantum tunneling to the incoherent coupling regime that may occur at finite temperatures^{38,40,43}. In particular, we are interested in a generic problem of the quantum-classical phase transition (PT) applied to macroscopic two-level systems^{45–49}.

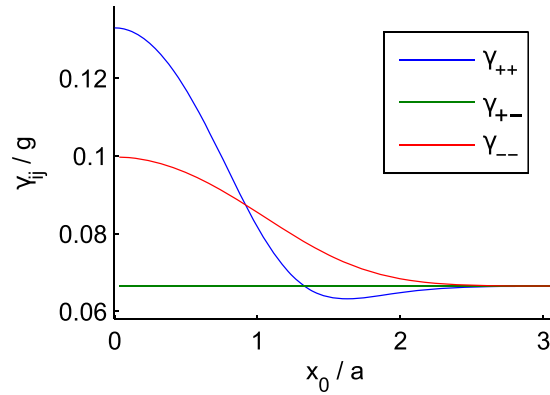


Figure 2. Dependences of the normalized matrix elements γ_{ij} $i, j \in \{+, -\}$ on the normalized half inter-well distance x_0/a ; a is a characteristic size of the condensate wavefunction.

Traditionally, studies in this field are limited by consideration of superconductor devices⁵⁰ where macroscopic quantum tunneling phenomena plays an essential role. In particular, it is worth to mention here the Schrödinger cat state formation⁵¹ and the design of quantum gates with superconductor qubits for quantum computing where a macroscopic quantum coherence for the phase is important⁵².

In this manuscript we specifically consider a couple of trapped exciton-polariton condensates in a high-Q GaAs microcavity. We take into account the driven-dissipative nature of the system, as well as the high temperature of the exciton-polariton gas. We go beyond the mean-field approximation adopted in the most part of theoretical works on exciton-polariton quantum fluids, and present the full phase diagram of the system. We shall consider a generalised model of exciton-polariton JJ that relates to so-called non-standard Bose-Hubbard models (see e.g refs 33, 53.) where the energy of polariton-polariton scattering contributes to the tunneling parameter matrix elements^{38–41, 43}. In order, we pay attention to the temperature dependent quantum critical phenomena occurring in the presence of macroscopic tunneling. We aim at formulation of the criteria for realisation of the quantum tunneling regime that is important for the realisation of the quantum annealing algorithms and exciton-polariton quantum gates. The influence of non-equilibrium effects involving the microcavity exciton polaritons possessing a finite lifetime is discussed as well.

The Quantum Phase Model

We consider a system of two spinless exciton-polariton condensates localised in lateral potential traps created in a planar semiconductor microcavity. The condensates are confined by a W-shape potential $U(x)$ possessing two minima at the points $\pm x_0$, see Fig. 1. Polaritons are pumped to the condensates from a reservoir of incoherent excitons. In this and next Section, we shall neglect the finite polariton lifetime and assume that the polariton gas is at the thermal equilibrium. We account for the polariton-polariton repulsion. In analogy to many body spin problems we introduce macroscopic pseudospins describing the polariton condensates⁵⁴. We note that a similar approach has been applied for the description of coherent phenomena in atomic gases⁵⁵.

We shall use the pseudo-spin operator representation for the Hamiltonian describing our exciton-polariton JJ model system that has a form (the details of the model are presented in the Supplementary Material):

$$\hat{H} = \alpha \hat{S}_z^2 + \beta \hat{S}_x^2 - B \hat{S}_x. \quad (1)$$

The coefficients in Eq. (1) characterize the tunnel coupling of two trapped condensates: the parameters α and β are proportional to the overlap integrals of real symmetric (Φ_+) and anti-symmetric (Φ_-) wavefunctions of two condensates that are $\gamma_{ij} = \int \Phi_i^2 \Phi_j^2 dx$, $i, j \in \{+, -\}$ —see Fig. 2 and Suppl. Materials; B is determined by difference of chemical potentials which obey stationary Gross-Pitaevskii (GP) equations for two trapped condensates.

It is important to note that the last term in Eq. (1) characterizes the familiar XY-model Hamiltonian considered in refs 28, 29. The second term in (1) introduces an additional part that has no analogy in the XY-Hamiltonian; it is proportional to $\cos(2\phi)$, where ϕ is the phase difference between two polariton condensates. This term vanishes in the limit $x_0/a \gg 1$, see Fig. 2 and Suppl. Materials^{31, 33, 35}.

It is convenient to introduce the pseudo-spin operators in a form

$$\hat{S}_x = s \cos \phi - \sin \phi \frac{d}{d\phi}, \quad (2a)$$

$$\hat{S}_y = s \sin \phi + \cos \phi \frac{d}{d\phi}, \quad (2b)$$

$$\hat{S}_z = -i \frac{d}{d\phi}, \quad (2c)$$

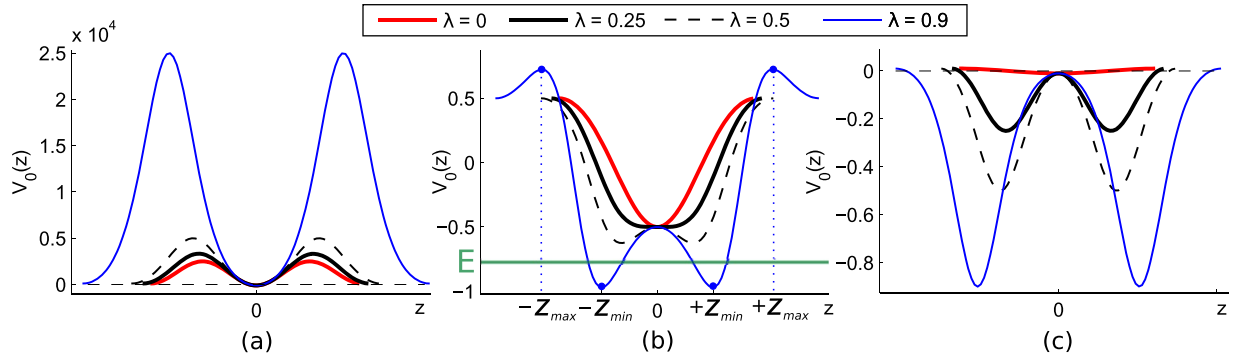


Figure 3. Effective dimension-less potential $V_0(z)$ for (a) $\Lambda = 100$, (b) $\Lambda = 0.5$, and (c) $\Lambda = 0.01$ as a function of the elliptic integral phase coordinate z . Points $\pm z_{min}$ and $\pm z_{max}$ in (b) correspond to global minima and maxima of the potential, respectively; E is the energy of the particle that experiences either quantum tunneling or thermal activation.

The operators defined in Eq. (2) obey familiar $SU(2)$ algebra commutation relations $[\hat{S}_i, \hat{S}_j] = i\epsilon_{ijk}\hat{S}_k$, $i, j, k = x, y, z$. After some straightforward calculations from (1) one can obtain

$$H = -(\alpha - \beta \sin^2 \phi) \frac{d^2}{d\phi^2} - \left(\beta \left(s - \frac{1}{2} \right) \sin 2\phi - B \sin \phi \right) \frac{d}{d\phi} - Bs \cos \phi - \beta s^2 \sin^2 \phi - \beta s \cos^2 \phi. \tag{3}$$

Thereafter we assume that both condensates are composed by macroscopically large numbers of particles, i.e. the $s = N/2 \gg 1$ is C - number. The general stationary Schrödinger equation with a Hamiltonian (3) writes:

$$(\alpha - \beta \sin^2 \phi) \frac{d^2 \Phi}{d\phi^2} + (\beta s \sin 2\phi - B \sin \phi) \frac{d\Phi}{d\phi} + (E + Bs \cos \phi + \beta s^2 \sin^2 \phi) \Phi = 0, \tag{4}$$

where $\Phi \equiv \Phi(\phi)$ is some 2π -periodic wavefunction that characterizes quantum phase properties⁵⁶. It is possible to eliminate the term with first derivative in Eq. (4). In order to find the explicit form of the function Φ , it is convenient to substitute it by:

$$\Phi(\phi) = \Psi(z) \exp \left[s \ln \operatorname{dn} z - \frac{\Lambda s}{2\sqrt{\lambda(1-\lambda)}} \arctan \left(\sqrt{\frac{\lambda}{1-\lambda}} \operatorname{cn} z \right) \right], \tag{5}$$

where $z = \int_0^\phi \frac{d\xi}{\sqrt{1-\lambda \sin^2 \xi}} = F(\phi, \lambda)$ is a new phase variable; $F(\phi, \lambda)$ is the incomplete elliptic integral of the first kind. In (5) we have introduced dimension-less parameters $\Lambda = \frac{B}{\alpha s}$, $\lambda = \frac{\beta}{\alpha}$. Inserting (5) into (4) we arrive to the familiar form of a Schrödinger equation

$$\alpha \frac{d^2 \Psi}{dz^2} + (E - V(z)) \Psi = 0. \tag{6}$$

This equation describes an effective particle with the mass $m = \frac{\hbar^2}{2\alpha}$ and energy E , that is confined by the potential $V(z) = \alpha s^2 V_0(z)$ with

$$V_0(z) = \frac{\left(\frac{1}{4} \Lambda^2 - \lambda(1-\lambda) \right) \operatorname{sn}^2 z - \Lambda \operatorname{cn} z}{\operatorname{dn}^2 z}. \tag{7}$$

The dependences of the trapping potential $V_0(z)$ on the phase variable z are shown in Fig. 3. The period of the functions is $4K(\lambda)$. The dependence of the λ -parameter on normalized half of the inter-well distance $\frac{x_0}{a}$ can be approximated by $\lambda = 0.5 \left(\exp \left[\frac{2x_0^2}{a^2} \right] - 1 \right)^{-1}$ by using variational approach, see Suppl. Materials. The well-known behaviour of the quantum phase mesoscopic JJ (that map to the XY-model^{28,29}) can be recovered from (1), (7) at $\lambda = 0$ and shown by red curves in Fig. 3. This limit corresponds to infinitely large inter-well distances, with $x_0 \rightarrow \infty$, Fig. 2. On the other hand, the λ -parameter exhibits a sharp increase at $\frac{x_0}{a} \ll 1$. Obviously, in this limit our exciton polariton JJ model based on the assumption of a relatively weak coupling between trapped condensates breaks down. Below we are focusing on λ -parameters which belong to the range of $0 < \lambda < 1$ and correspond to

the moderate values of $\frac{x_0}{a}$ such as $\frac{x_0}{a} \geq 0.45$. The analysis of the quantum phase can be performed in three domains determined by vital Λ -parameter values⁵⁶.

Rabi regime $\Lambda \gg 1$. In this limit the trapping potential can be approximated by $V_R(z) = \frac{1}{4}\Lambda^2 sd^2 z$. Physically, for any value of λ -parameter belonging to the domain $0 < \lambda < 1$ the system exhibits (Rabi) oscillations for the phase. In particular, small amplitude oscillations which are inherent to familiar Rabi regime can be achieved for negligible λ -see Fig. 3a and ref. 56.

Fock regime $\Lambda \ll 1/N^2$. In purely quantum limit $\Phi(\phi) \rightarrow (2\pi)^{-1/2}$. In this regime, when inequality $\Lambda \ll \lambda < 1$ is held, Eq. (6) transforms to the Mathieu equation that is characterised by the set of eigen states consisting of all Mathieu functions.

Josephson regime $1/N^2 \ll \Lambda < 1$. This regime corresponds to the intermediate case between Rabi and Fock limits-see Fig. 3b. The behavior of the phase depends on the ratio between the parameters Λ and λ . If $\Lambda \geq 2\lambda$ the potential $V_0(z)$ possesses only one minimum at $z=0$ and $V(0) = -\Lambda$.

In the opposite limit, for $\Lambda < 2\lambda$, the effective quantum “particle” described by Eq. (6) is trapped at the two minima of $V_0(z)$ that correspond to the W -like potential with coordinates $z_{min} = \pm cn^{-1} \frac{\Lambda}{2\lambda}$ and appearing for both of Josephson and Fock regimes, see Fig. 3b,c. The depth of the potential minima depends on the λ parameter. It is interesting to note that for $\Lambda > 2(1-\lambda)$ the potential $V_0(z)$ possesses a local minimum at $\pm 2K(\lambda)$, see Fig. 1b.

Annealing problem versus Quantum-classical PT's

Quantum-classical PT's. Experimentally, exciton-polariton condensates are being observed at elevated temperatures, up to the room temperature in wide-gap semiconductor microcavities^{1,2}. At high temperatures the validity of the quantum coherent treatment of the Josephson problem is limited. In this section, we study the limits of validity of the quantum approach which also set the limits of the system suitability for quantum annealing²⁵.

To be more specific we consider the tunneling in an effective W -like potential shown in Fig. 3b. We assume the thermal equilibrium condition to be fulfilled for an ensemble of exciton-polaritons at finite temperatures T , that would correspond to a hypothetical case of polaritons with the infinite life-time. We note in this connection that in the recent experiments⁴⁴ the measured polariton lifetime was as long as 275 ps, which would be sufficient to justify the above approximation.

A transition between two stable states (say, between points $-z_{min}$ and $+z_{min}$ in Fig. 3b) can happen either through the quantum tunneling or, in classical way, due to the thermal activation. Below we show that the crossover between these two regimes may possess features of either a first (1st)- or second (2nd)-order phase transition. Obviously, at high temperatures such as $k_B T \geq \Delta V$ (ΔV is the height of the barrier between two states with minimum of potential energy) the particle jumps over the barrier governed by the thermoactivation (Arrhenius) escape rate $\Gamma_T \sim e^{-\Delta V/k_B T}$ ⁴⁷. This process is inherent to the classical (thermal) annealing problem²⁵. In the “low temperature” limit $k_B T \ll \Delta V$ polaritons undergo quantum tunneling through the barrier with a vanishing rate

$$\Gamma \sim e^{-S_{min}/\hbar}, \quad (8)$$

where S_{min} is minimal value of the action, that excludes realisation of the quantum annealing scheme. At the crossover temperature $T_c = \hbar \Delta V / k_B S_{min}$ the matching condition for the tunnelling rates may be anticipated.

Our description is based on imaginary time path integral approach⁵⁰. The imaginary-time action obtained within the WKB method approaches as

$$S(E) = \oint \left(\frac{1}{2} m \dot{z}^2 + V(z) \right) d\tau. \quad (9)$$

At the temperatures below the barrier height ΔV Eq. (9) enables one finding the escape rate Γ_T ⁴⁵

$$\Gamma_T \sim \int_0^{\Delta V} e^{-(E+k_B TS(E)/\hbar)/k_B T} dE = \int_0^{\Delta V} e^{-F/k_B T} dE, \quad (10)$$

where

$$F = E + k_B TS(E)/\hbar \quad (11)$$

plays role of the free energy of the system. The trajectories which minimize the action S_T obey the classical equation of motion $m\dot{z} = \frac{dV}{dz}$ written for the thermon “particle” that oscillates within the inverted potential $-V(z)$. Periodic solutions of this equation satisfy

$$\frac{1}{2} m \dot{z}^2 = V(z) - E(\tau_p), \quad (12)$$

where $\tau_p = \hbar/k_B T$ is a thermon period corresponding to the energy $E(\tau_p)$ and shown in Fig. 3b;

$$\tau_p(E) = \sqrt{2m} \int_{z_1(E)}^{z_2(E)} \frac{dz}{\sqrt{V(z) - E}}. \quad (13)$$

In (13) the $z_{1,2}(E)$ are the turning points, see Fig. 3b. Equations (12,13) taken at the energy $E=0$ and temperature $T=0$ characterize the instanton solution with an infinite period. Remarkably in this case from (10) one can immediately obtain Eq. (8) that yields the escape rate in the quantum domain.

Combining (9) with (12) we arrive to

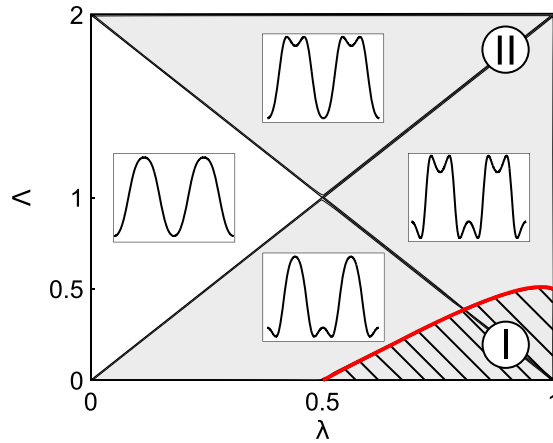


Figure 4. Diagram of the phase boundary for the 1st- and 2nd-order PT's in Λ, λ -parameters plane. The PEL's are shown in the windows.

$$S_T = 2\sqrt{2m} \int_{z_1(E)}^{z_2(E)} \sqrt{V(z) - E} dz + E\tau_p(E). \tag{14}$$

To reveal the thermodynamic properties of the system it is necessary to consider small amplitude oscillations at the bottom, $z = 0$, of the inverted potential $-V(z)$. The action in this case reads:

$$S_0 = \Delta V\tau_p(E). \tag{15}$$

The expansion of the potential $V(z)$ into a series and excluding the constant value $V(0)$ gives:

$$V(z) = \alpha s^2(c_2 z^2 + c_4 z^4 + o(z^4)), \tag{16}$$

where c_2 and c_4 are coefficients defined as

$$c_2 = \frac{1}{4}\Lambda^2 - \frac{2\lambda - 1}{2}\Lambda - \lambda(1 - \lambda), \tag{17}$$

$$c_4 = \frac{2\lambda - 1}{12}\Lambda^2 - \frac{16\lambda^2 - 16\lambda + 1}{24}\Lambda - \frac{\lambda(1 - \lambda)(2\lambda - 1)}{3}. \tag{18}$$

In particular, if the inverted potential $-V(z)$ has the form $z^2 - z^4$ ($c_2 < 0, c_4 > 0$) the 2nd order phase transition occurs. If $-V(z)$ behaves as $z^2 + z^4$ ($c_2 < 0, c_4 < 0$) the 1st order phase transition take place. The phase boundary between the 1st and 2nd order phase transitions is determined by the relation

$$\Lambda = \frac{1 - 16\lambda + 16\lambda^2 + \sqrt{1 + 32\lambda - 32\lambda^2}}{4(2\lambda - 1)}. \tag{19}$$

We summarize our results in Fig. 4. An inset demonstrates various types of phase potentials $V_0(z)$ inherent to our exciton-polariton JJ model. The 1st order PT occurs for two type of potentials in the shaded region bounded by bold (red) curve. Second order PT's appear for the potential landscapes taken from the dark area. The crossover temperature $T_c^{(2)} = \hbar\omega_0/2\pi k_B$ of 2nd-order PT transition is

$$T_c^{(2)} = T_0 \sqrt{\lambda(1 - \lambda) + (2\lambda - 1)\frac{\Lambda}{2} - \frac{1}{4}\Lambda^2}, \tag{20}$$

where $\omega_0 = \frac{2\alpha s}{\hbar} \sqrt{\lambda(1 - \lambda) + \frac{1}{2}(2\lambda - 1)\Lambda - \frac{1}{4}\Lambda^2}$ is a frequency of small oscillations of the thermon “particle” near the bottom of inverted potential, $T_0 = \alpha N/2\pi k_B$ is a characteristic temperature that inherent to exciton polariton system. The T_0 implies important time scale $\tau_0 = 2\pi\hbar/\alpha N$ that can be understood as thermon particle “lifetime”. Notably, as it is follows from (20) there is no barrier at $z = 0$ for $\Lambda \geq 2\lambda$ —see the white domain in Fig. 4.

In Fig. 5a we represent the results exhibiting 1st-order PT inherent to narrow shadow domain in Fig. 4 where discontinuity of the derivative dS/dT occurs. It is clearly seen that the first derivative of S_{min} is discontinuous in this case and the dependence of the normalized thermon period τ_p/τ_0 on the energy E is non-monotonic, see the inset in Fig. 5a. The critical temperature $T_c^{(1)}$ belongs to the temperature domain $T_{min} < T_c^{(1)} < T_{max}$ and it can be found out numerically by solving Eqs (13–15) in the particular case of $S_T = S_0$.

Analytically, the critical temperature $T_c^{(1)}$ may be estimated from $T_c^{(1)} = \hbar\Delta V/k_B S_{inst}^{(1)}$, where S_{inst} is an instanton action that can be represented as $S_{inst} = S(E_{min})$. After some straightforward calculations for S_{inst} we obtain

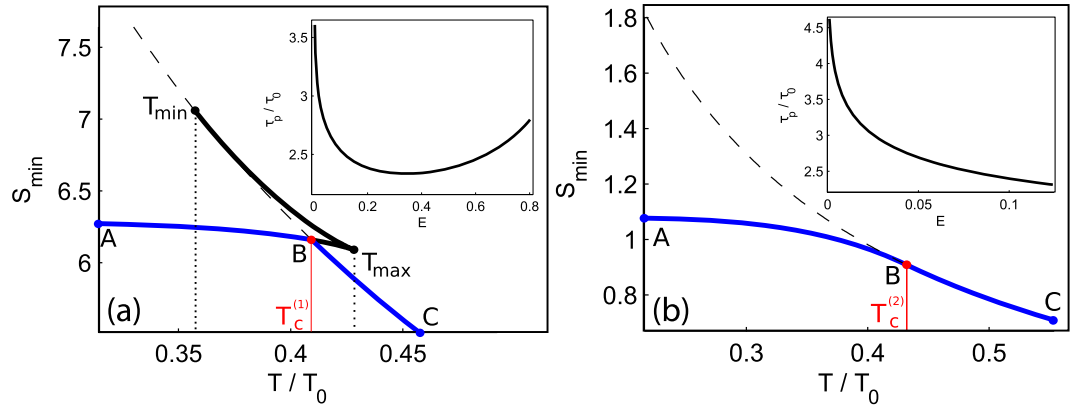


Figure 5. Dependences of the minimal action S_{min} (ABC-blue) curve) taken in sh units as a function of the normalized temperature T/T_0 for (a) 1st-order PT, $\lambda=0.9$, $\Lambda=0.1$; and, (b) 2nd-order PT, $\lambda=0.5$, $\Lambda=0.5$; the solid (bold) line corresponds to the thermon action, S_T ; the dashed line corresponds to the thermodynamic action, $S_0 = \hbar\Delta V/k_B T$, $S_{min} = \min\{S_0, S_T\}$. The inset shows the dependences of normalized thermon period τ_p/τ_0 on energy E expressed in αs^2 units.

$$S_{inst} = S(E_{min}) = 2s\hbar \left[\ln \frac{2\sqrt{\lambda} + \sqrt{4\lambda^2 - \Lambda^2}}{2\sqrt{\lambda} - \sqrt{4\lambda^2 - \Lambda^2}} - \frac{\Lambda}{\sqrt{\lambda(1-\lambda)}} \arctan \left(\frac{\sqrt{(1-\lambda)(4\lambda^2 - \Lambda^2)}}{\Lambda} \right) \right] \quad (21)$$

Figure 5b displays 2nd-order PT from quantum (solid bold line of S_T) to thermal (classical) regimes—dashed bold line of S_0 . The crossover occurs at the critical temperature $T_c^{(2)}$ where $S_T = S_0$ and $E = E_0$. The inset demonstrates a monotonic dependence of the normalized thermon period τ_p/τ_0 on energy E that is inherent to second-order phase transition. Closest to the critical point with energy $E = E_0$ the thermon undergoes small amplitude oscillations.

Remarkably, from Fig. 5 it is clearly seen that at the temperatures sufficiently below the critical temperatures T_c the action S_{min} is temperature independent that corresponds to the quantum regime of macroscopic tunneling. The connection with phenomenological Landau theory of PT’s⁵⁷ can be obtained by introducing the “order parameter” P that is⁴⁵

$$P = \sqrt{\frac{V(0) - E}{\Delta V}} \quad (22)$$

Taking into account Eq. (11) for normalized free energy $F(P)$ one can obtain

$$\frac{F(P)}{\Delta V} = 1 + (\theta - 1)P^2 + \theta\eta P^4 + O(P^6), \quad (23)$$

where $\eta = 3c_4(\Lambda - 2\lambda)^2/32c_2^2\lambda$ and $\theta = T/T_c^{(2)}$ is normalised temperature parameter. It is important that sign of second term in Eq. (23) is completely determined by sign of c_4 -coefficient, see (18), that implies whether 1st-, or 2nd-order PT occurs in the system.

Thus, P -parameter describes features of potential shape for the “particle” possessing energy E and characterizing PT in the system according to Landau theory⁵⁷—see Fig. 3b. Figure 6 shows the behaviour of the introduced order parameter. One can see that the phases corresponding to the quantum tunneling and classical thermal activations are separated by the second order phase transition.

In the optical experiments one usually has a better control of the exciton-polariton density than their effective temperature, see e.g. refs 1, 2. For instance, the density of polariton gas can be changed by varying the optical pump intensity. In Fig. 7 we plot a numerically calculated critical temperature of the 1st and 2nd order PTs as a function of the Λ -parameter for experimentally accessible semiconductor JJ samples. The bold (green) line corresponds to the analytical solution obtained with Eq. (21). Since the Λ -parameter is inversely proportional to the density of the exciton-polariton gas (and the blue-shift of the energy of the corresponding photoluminescence peak) Fig. 7 establishes an important relation between the critical temperatures discussed in the paper and the relevant exciton polariton densities.

Now let us consider the decay of the state of the system that corresponds to the upper minimum of the potential $V(z)$ located at $\pm 2K(\lambda)$ in Fig. 3b and exists for $\Lambda > 2(1 - \lambda)$. Physically, the decay takes place because of the tunneling of our effective particle through the barrier located at one of the points $z_{max} = \pm \text{cn}^{-1}\left(-\frac{2(1-\lambda)}{\Lambda}\right)$. By expanding the potential $V(z)$ in the vicinity of z_{max} it is possible to show that only the 2nd-order PT with a temperature $T_c^{(2)} = (T_0/2)\sqrt{\frac{\Lambda^2}{1-\lambda} - 4(1-\lambda)}$ may take place in this case.

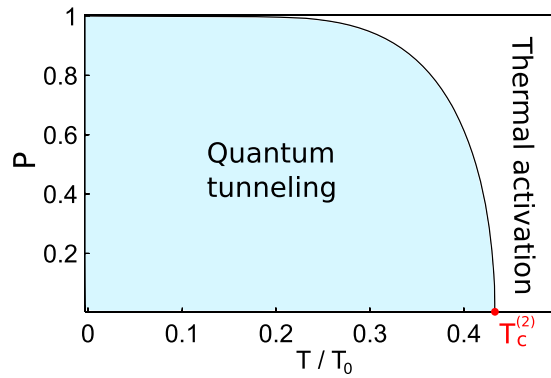


Figure 6. The dependence of the P -parameter on the normalized temperature T/T_0 . The parameters λ, Λ are the same as in Fig. 5b.

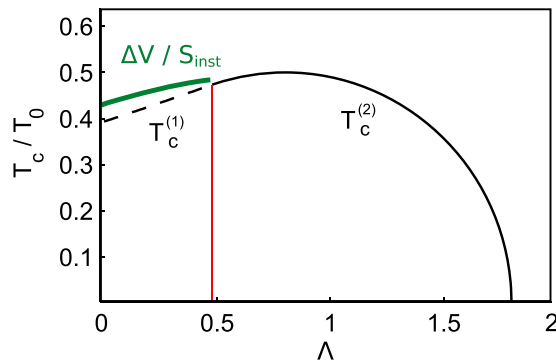


Figure 7. The dependence of the normalized critical temperature T_c/T_0 as a function of the parameter Λ . The bold (green) line corresponds to the analytical expression for $T_c^{(1)}$ given by Eq. (21).

Annealing. Nowadays simulated annealing (SA) algorithm is at the heart of the optimization problem in computer science, see e.g. ref. 58. In particular, it enables to solve so-called NP -hard optimization problems that is met in our life frequently; an example, we refer here to the traveling salesman problem, see e.g. ref. 59. From the point of view of the physical implementation, the optimization algorithm implies searching of a global minimum for PEL that relays to N particle spin system oriented randomly²⁵. According to the SA approach the minimum can be achieved by physical system as a result of the deep cooling. Apart from SA, quantum annealing (QA) uses the quantum tunneling option to achieve a global minimum. In some aspects QA algorithm is relevant to the so-called adiabatic quantum computing scheme⁶⁰. Although in this paper we are not aiming at detail investigation of various annealing schemes, some of their features become evident from our previous analysis.

Actually, at high enough temperatures, the system may visit the higher-energy eigen states by means of the thermal activation and due to thermal fluctuations, see Fig. 1. Certainly, at zero temperature, being at the full thermodynamic equilibrium state, one can find the configuration of the spin system at PEL minimum possessing also minimum of its free energy F and action S_{min} , respectively, see Eqs (11,23). Clearly, the last one corresponds to the implementation of QA algorithm when system undergoes quantum tunneling instead of thermal activation. The transition between these two scenarios, in fact, reflects the nature of SA scheme that lies in the crossover from the thermal (classical) to the quantum annealing regime.

From the practical point of view, it is instructive to estimate the time that is required for the system to perform the computation. Obviously this time is limited by characteristic tunneling time, or by the characteristic hopping time. Here we estimate this time simply as

$$t_T = \hbar/\Gamma_T. \tag{24}$$

Obviously, the characteristic time scale t_T depends on the temperature of the system. At $T=0$, where only the QA is possible, from (24) we obtain

$$t_0 = e^{S_{min}/\hbar}. \tag{25}$$

One can see that the parameter t_0 defines limiting (minimal) time required to perform QA for our toy optimization model. Notably, this time depends on the number of particles as $t_0 = e^{N\gamma'}$, where γ' is some constant. Since relation $S_T > S_{min}$ is still valid up to the temperatures of PT we have $t_T > t_0$ in the same limit. Thus, from (24) and (25) immediately follows that improvement of the annealing algorithm in the quantum domain strongly depends

on the particle number N and governed by the ratio $t_T/t_0 = e^{(S_T - S_{min})/\hbar}$ which depends on the effective action difference taken at a given temperature T ; this difference clearly seen from Fig. 5a for the 1st order PT problem where thermal and quantum regimes coexist.

Slightly above the critical temperature T_c the thermal (classical) SA algorithm is realised in our system. At relatively high temperatures it does not guarantee the system relaxation to the global minimum. Moreover, some non-equilibrium processes can occur in this case and the model used here may be no more valid (see next Section). The predictions of the present model must be valid in the vicinity of critical point and below.

Let us briefly discuss methods of the experimental study of the quantum-classical PT for the polariton JJ's. Our estimations show that, for the experimentally accessible polariton interaction strength of $\alpha N = 0.6 \text{ meV}$, characteristic of narrow-band semiconductor samples, T_0 is about 1.1 K that corresponds to the thermal effective lifetime of $\tau_0 \approx 7 \text{ ps}$. The value of T_0 is comparable with a typical temperature of a BEC, or, with temperature of the Berezinsky-Kosterlitz-Thouless PT predicted for the dilute weakly interacting exciton-polariton gas at thermal equilibrium^{1,2}. Some further enhancement of T_0 may be achieved by the increase of the optical pumping intensity and varying the detuning of exciton and photon modes in a microcavity⁴⁴.

PT's in the presence of dissipation

Now let us consider the exciton polariton JJ accounting for the finite exciton polariton lifetime τ_{pol} . The finite radiative lifetime is an important characteristic of any polariton system and, strictly speaking, can never be ignored. Obviously, in order to allow for the Josephson oscillations, the characteristic time τ_0 that is responsible for quantum tunneling effects should be shorter than all characteristic times describing non-equilibrium processes in the exciton-polariton gas, including the radiative decay. Hence,

$$\tau_0 \ll \tau_{pol}. \quad (26)$$

The condition (26) is fulfilled in the experimental work⁴⁴, in particular. Here we examine a different situation namely, the case where the exciton polariton lifetime τ_{pol} is comparable with τ_0 . Note that this situation is realized the multiple experiments dealing with non-equilibrium exciton polariton condensates, see e.g. refs 1, 2, 16–18.

To be more specific in what follows we shall consider the influence of the dissipation on the exciton polariton JJ quantum phase properties in the adiabatic limit⁶¹. We start from GP equations obtained from (see Supplementary equation (S5)) for the mean fields $\psi_{1,2} = \langle \hat{\psi}_{1,2} \rangle$ at $\Gamma = 0$ ($B = G$), which read as

$$i\hbar\dot{\psi}_{1,2} = -i\kappa\psi_{1,2} + (A|\psi_{1,2}|^2 + 2C|\psi_{2,1}|^2)\psi_{1,2} - (B/2 - C\psi_{1,2}^*\psi_{2,1})\psi_{2,1}. \quad (27)$$

In (27) we have introduced the dissipation term with $\kappa \simeq \hbar/\tau_{pol}$. Defining new variables $\Psi_{1,2}$ as $\psi_{1,2} = \Psi_{1,2}\exp(-\kappa t/\hbar)$ for the mean field pseudo-spin components (see Supplementary equation (S6)). We obtain from (27)

$$\begin{aligned} \dot{S}_x &= -2\alpha'(t)S_zS_y; \\ \dot{S}_y &= 2(\alpha'(t) - \beta'(t))S_zS_x + S_z; \\ \dot{S}_z &= 2\beta'(t)S_xS_y - S_y; \end{aligned} \quad (28)$$

Here we have introduced the dimensionless time $t' = tB/\hbar$.

Set of Eq. (28) describes the dynamics of normalized mean field pseudo-spin parameters on the Bloch sphere with $S_x^2 + S_y^2 + S_z^2 = 1$. Equation (28) look similar to those written for a non-dissipative system but with the time dependent parameters $\alpha'(t) = (1/\Lambda)\exp(-2\kappa't')$, $\beta'(t) = (\lambda/\Lambda)\exp(-2\kappa't')$, $\kappa' = \kappa/B$ ⁶². Taken out the dissipation, Eq. (28) possesses a bifurcation point $\lambda/\Lambda = 1/2$ that corresponds to the solid black curve in Fig. 3b.

In Fig. 8a we plot the phase difference between the condensates $\phi = \arctan(-S_y/S_x)$ as a function on time. A non-dissipative system has two different regimes depending on the values of the β -parameter, that are blue (labeled as 1) and red (labeled as 3) curves in Fig. 8, respectively. The blue curve is plotted for the case of $\beta' > 1/2$ and it corresponds to the quantum regime—see Fig. 8b. Contrary, the red curve describes the phase between two condensates below the threshold ($\beta' < 1/2$) that corresponds to the absence of the barrier.

In the presence of dissipation (solid black curve in Fig. 8a) the phase of exciton-polariton JJ starts from one of the potential minima. We assume here that the temperature of the system is not sufficient for thermal activation and the quantum tunneling is possible. The system evolves adiabatically and then crosses the critical value $\beta = 1/2$ due to the decrease of the total number of particles caused by the radiative decay. The final (temporal) state represents the Josephson or, Rabi oscillation regime.

Figure 8b and c demonstrate the suppression of W -like potential and the relevant enhancement of the reduced thermal period τ_p/τ_0 which occurs at switching time $t_{sw} = 11.5 \text{ ps}$ for $\tau_{pol} \sim \hbar/\kappa = 10 \text{ ps}$, respectively.

Thus, behavior of the phase in the presence of dissipation showed in Fig. 8 is characteristic of an established non-equilibrium PT from the regime where tunneling is possible to the regime where tunneling is suppressed. However, this regime found at $t > t_{sw}$ cannot be interpreted immediately as the classical one. Actually, the adiabaticity condition reads⁶¹:

$$\frac{1}{\omega^2(t)} \left| \frac{d\omega}{dt} \right| \ll 1. \quad (29)$$

where $\omega(t) = B\sqrt{(1 - 2\beta'(t))(1 - 2\beta'(t) + 2\alpha'(t))}/\hbar$ is the frequency of small oscillations slowly depending on time⁶². The solution for the phase in this case can be approximated by

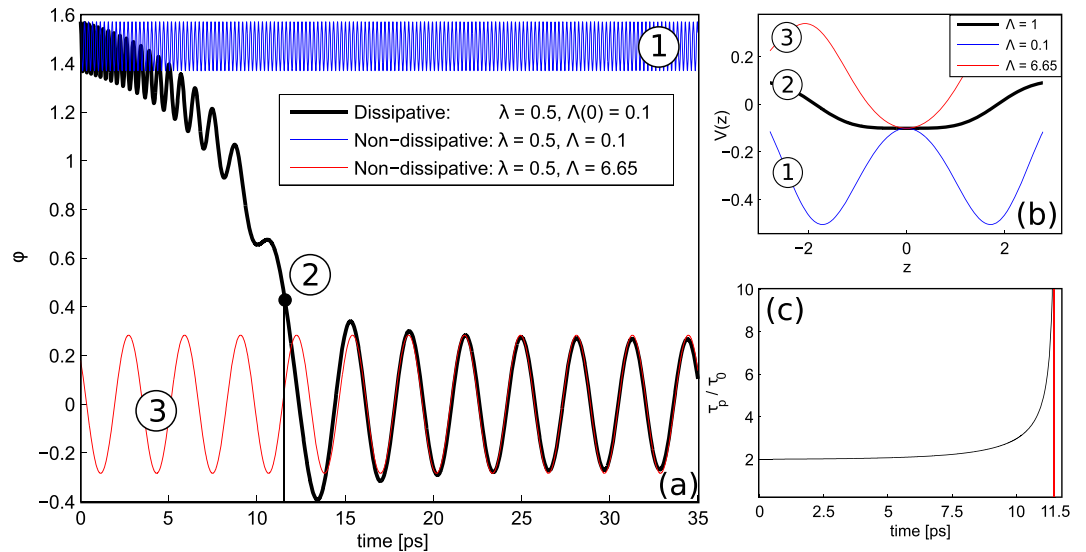


Figure 8. (a) Normalized phase difference as a function of time; (b) effective potential vs phase parameter z for red, black and blue curves, respectively, and (c) reduced thermion period τ_p/τ_0 vs time for $\kappa/\hbar = 0.1$ THz. Initial conditions are $S_x(0) = S_y(0) = 0$, $S_z(0) = 1$, and $\phi(0) = \pi/2$, respectively.

$$\phi(\tau) \approx \frac{A}{\omega(\tau)} \cos(\omega(\tau)\tau), \quad (30)$$

where τ is the time elapsed after the oscillation sets in, and A is the amplitude of oscillations at $\tau = 0$. At large enough times, $\omega(t) \approx B/\hbar$ and permanent Rabi oscillations for the JJ phase ϕ are established, see Fig. 8a and ref. 63. To distinguish between the quantum and classical character of these oscillations, a purely quantum approach to the problem should be considered. It will be in the scope of our further research.

Conclusion

We have studied theoretically the coupling of two spatially separated trapped exciton-polariton condensates at finite temperatures and accounting for the dissipation. We demonstrate the crossover from thermal to quantum annealing regime for a model system of two condensates localised by a W-shape potential. Second regime is classical one and characterizes thermal activation. The transition between these two regimes exhibits universal features of the 1st or 2nd order PTs which can be interpreted as PT between classical and quantum regimes. It is important that critical temperature of transition depends on some characteristic temperature parameter T_0 (see e.g. (20)) that that is governed by the polariton-polariton interaction length (so-called blue shift) αN . It is expected that at the temperatures sufficiently higher than T_0 the exciton-polariton JJ device operates in classical way. In this case the simulated thermal annealing algorithm might be implemented.

The influence of dissipation effects originating from the radiative decay of polaritons by photon tunneling through the Bragg mirrors is revealed by our analysis. The observation of quantum tunneling processes only becomes possible within short time intervals where the dissipation cannot essentially affect the system. Otherwise, after some time interval the dissipation leads to crossover in the phase dynamics and it damages the W-potential as a whole, see Fig. 8. In this case permanent Rabi oscillations of JJ phase occurs within the adiabatic approach. To reveal either quantum or classical nature of these oscillations it is necessary to study the fluctuations of the exciton-polariton system beyond the semiclassical approach. For moderate dissipation rates and at temperatures (or relevant polariton gas densities) sufficiently below the temperature of T_0 the exciton-polariton JJ device is suitable for various applications where the quantum tunneling effect is crucial.

We note that the quantum tunneling effect may be used for designing exciton polariton phase qubits similar to superconductor devices, but in the optical wavelength domain⁵². Actually, two minima located at the points $-z_{min}$ and $+z_{max}$ of W-shape quantum phase potential in Fig. 3b can be used for setting the exciton polariton qubit states $|0\rangle$ and $|1\rangle$ similarly to superconductor flux qubits. However, in our case such qubits may be tailored by the external optical or electrical pump. As a result, QA problem can be experimentally solved with use of the polariton-based qubits⁶⁴.

References

- Sanvitto, D. & Timofeev, V. *Exciton Polaritons in Microcavities*, vol. 172 of *Springer Series in Solid-State Sciences* (Springer-Verlag Berlin Heidelberg, 2012).
- Guillet, T. & Brimont, C. Polariton condensates at room temperature. *Comptes Rendus Physique* **17**, 946 (2016).
- Bhattacharya, P. *et al.* Room temperature electrically injected polariton laser. *Phys. Rev. Lett.* **112** (2014).
- Schneider, C., Rahimi-Iman, A. & Kim, N. Y. *et al.* An electrically pumped polariton laser. *Nature* **497** (2013).
- Niemietz, D., Schmutzler, J. & Lewandowski, P. Experimental realization of a polariton beam amplifier. *Phys. Rev. B* **93** (2016).
- Amo, A. *et al.* Exciton-polariton spin switches. *Nature Photonics* **4**, 361 (2010).

7. Ballarini, D., Giorgi, M. D. & Cancellieri, E. *et al.* All-optical polariton transistor. *Nature Comms* **4**, 1778 (2013).
8. Sturm, C., Tanese, D. & Nguyen, H. S. *et al.* All-optical phase modulation in a cavity-polariton mach-zehnder interferometer. *Nature Comms* **5**, 32 (2014).
9. Liew, T. C. H., Kavokin, A. V. & Shelykh, I. A. Optical circuits based on polariton neurons in semiconductor microcavities. *Phys. Rev. Lett.* **101** (2008).
10. Byrnes, T., Kim, N. Y. & Yamamoto, Y. Exciton-polariton condensates. *Nat. Phys* **10**, 803 (2014).
11. Lai, Y.-Y. *et al.* Crossover from polariton lasing to exciton lasing in a strongly coupled znO microcavity. *Scientific Reports* **6**, 20581 (2016).
12. Carusotto, I. & Ciuti, C. Quantum fluids of light. *Rev. Mod. Phys.* **85**, 299 (2013).
13. Amo, A. *et al.* Collective fluid dynamics of a polariton condensate in a semiconductor microcavity. *Nature* **457**, 291 (2009).
14. Lagoudakis, K. G. *et al.* Quantized vortices in an exciton-polariton condensate. *Nat. Phys.* **4**, 706 (2008).
15. Lagoudakis, K. G. *et al.* Observation of half-quantum vortices in an exciton-polariton condensate. *Science* **326**, 974 (2009).
16. Sich, M. *et al.* Observation of bright polariton solitons in a semiconductor microcavity. *Nat. Photon.* **6**, 50 (2011).
17. Abbarchi, M. *et al.* Macroscopic quantum self-trapping and josephson oscillations of exciton polaritons. *Nat. Phys.* **9**, 275 (2013).
18. Lagoudakis, K. G., Pietka, B., Wouters, M., André, R. & Deveaud-Plédran, B. Coherent oscillations in an exciton-polariton josephson junction. *Phys. Rev. Lett.* **105**, 120403 (2010).
19. Dominici, L., Colas, D. & Donati, S. *et al.* Ultrafast control and rabi oscillations of polaritons. *Phys. Rev. Lett.* **113** (2014).
20. Demirchyan, S. S., Chestnov, I. Y., Alodjants, A. P., Glazov, M. M. & Kavokin, A. V. Qubits based on polariton rabi oscillators. *Phys. Rev. Lett.* **112**, 196403 (2014).
21. Pagel, D., Fehske, H., Sperling, J. & Vogel, W. Strongly entangled light from planar microcavities. *Phys. Rev. A* **86**, 052313 (2012).
22. Kyriienko, O. & Liew, T. C. H. Exciton-polariton quantum gates based on continuous variables. *Phys. Rev. B* **93** (2016).
23. Solnyshkov, D. D., Bleu, O. & Malpuech, G. All optical controlled-not gate based on an exciton-polariton circuit. *Superlattices and Microstructures* **83**, 466–475 (2015).
24. Santoro, G. & Tosatti, E. Optimization using quantum mechanics: quantum annealing through adiabatic evolution. *J. Phys. A* **39**, R393 (2006).
25. Das, A. & Chakrabarti, B. Quantum annealing and analog quantum computation. *Rev. of Mod. Phys.* **80**, 1061 (2008).
26. Graß, T. & Lewenstein, M. Hybrid annealing using a quantum simulator coupled to a classical computer. *LANL arXiv* 1611.09729v1 (2016).
27. Yan, K., Byrnes, T. & Yamamoto, Y. Kinetic monte carlo study of accelerated optimization problem search using bose-einstein condensates. *Progress in Informatics* **8**, 39 (2011).
28. Ohadi, H. *et al.* Nontrivial phase coupling in polariton multiplets. *Phys. Rev. X* **6**, 031032 (2016).
29. Berloff, N. *et al.* Realizing the xy hamiltonian in polariton simulators. *arXiv* 1607.06065v1 (2016).
30. Barone, A. & Paterno, G. *Physics and Applications of the Josephson Effect* (Wiley, New York, 1982).
31. Raghavan, S., Smerzi, A., Fantoni, S. & Shenoy, S. Coherent oscillations between two weakly coupled bose-einstein condensates: Josephson effects, π oscillations, and macroscopic quantum self-trapping. *Phys. Rev. A* **59**, 620 (1999).
32. Leggett, A. Bose-einstein condensation in the alkali gases: Some fundamental concepts. *Rev. Mod. Phys.* **73**, 307 (2001).
33. Gati, R. & Oberthaler, M. A bosonic josephson junction. *J. Phys. B: At. Mol. Opt. Phys.* **40**, 61 (2007).
34. Alodjants, A., Arakelian, S., Bagayev, S., Egorov, V. S. & A. Yu, L. Josephson dynamics for coupled polariton modes under the atom-field interaction in the cavity. *Appl. Phys. B* **89**, 81 (2007).
35. Chuchem, M. *et al.* Quantum dynamics in the bosonic josephson junction. *Phys. Rev. A* **82**, 053617 (2010).
36. Shin, Y. *et al.* Optical weak link between two spatially separated bose-einstein condensates. *Phys. Rev. Letts.* **95**, 170402 (2006).
37. Morsch, O. & Oberthaler, M. Dynamics of bose-einstein condensates in optical lattices. *Rev. Mod. Phys.* **78**, 180 (2006).
38. Shelykh, I., Solnyshkov, D., Pavlovic, G. & Malpuech, G. Josephson effects in condensates of excitons and exciton polaritons. *Phys. Rev. B* **78** (2008).
39. Lai, C. W. *et al.* Coherent zero-state and π -state in an exciton-polariton condensate array. *Nature* **450** (2007).
40. Borgh, M., Keeling, J. & Berloff, N. Spatial pattern formation and polarization dynamics of a nonequilibrium spinor polariton condensate. *Phys. Rev. B* **81** (2010).
41. Sarchi, D., Carusotto, I., Wouters, M. & Savona, V. Coherent dynamics and parametric instabilities of microcavity polaritons in double-well systems. *Phys. Rev. B* **77** (2008).
42. Read, D., Rubo, Y. G. & Kavokin, A. V. Josephson coupling of bose-einstein condensates of exciton-polaritons in semiconductor microcavities. *Phys. Rev. B* **81** (2010).
43. Aleiner, I. L., Altshuler, B. & Rubo, Y. G. Radiative coupling and weak lasing of exciton-polariton condensates. *Phys. Rev. B* **85** (2012).
44. Sun, Y. *et al.* Bose-einstein condensation of long-lifetime polaritons in thermal equilibrium. *Phys. Rev. Lett.* **118**, 016602 (2017).
45. Chudnovsky, E. M. & Garanin, D. A. First- and second-order transitions between quantum and classical regimes for the escape rate of a spin system. *Phys. Rev. Letts.* **79**, 4469 (1997).
46. Caldeira, A. O. & Leggett, A. J. Quantum tunnelling in a dissipative system. *Ann. Phys. (N.Y.)* **149**, 374 (1983).
47. Larkin, A. I. & Ovchinnikov, Y. N. Decay of the supercurrent in tunnel junctions. *Pis'ma Zh. Eksp. Teor. Fiz* **37**, 382 (1983). *Sov. JETP Letts.*, issue 37/7, p. 322 (2003).
48. Riseborough, P. S., Hanggi, P. & Freidkin, E. Exact results for a damped quantum-mechanical harmonic oscillator. *Phys. Rev. A* **32**, 489 (1985).
49. Zhang, Y. & Muller-Kirsten, H. J. W. Periodic instanton method and macroscopic quantum tunneling between two weakly linked bose-einstein condensates. *Phys. Rev. A* **64** (2001).
50. Ankerhold, J. *Quantum Tunneling in Complex Systems. The Semiclassical Approach* (Springer-Verlag Berlin Heidelberg, 2007).
51. Leggett, A. J. Schrodinger's cat and her laboratory cousins. *Contemp. Phys.* **25**, 583 (1984).
52. Makhlin, Y., Schön, G. & Shnirman, A. Quantum-state engineering with josephson-junction devices. *Rev. Mod. Phys.* **73**, 357 (2001).
53. Dutta, O. *et al.* Non-standard hubbard models in optical lattices: a review. *Rep. Prog. Phys.* **78** (2015).
54. Owerre, M. B. & Paranjape, S. A. Macroscopic quantum tunneling and quantum-classical phase transitions of the escape rate in large spin systems. *Phys. Rep.* **546** (2015).
55. Hammerer, K., Sorensen, A. & Polzik, E. Quantum interface between light and atomic ensembles. *Rev. Mod. Phys.* **82**, 1041 (2010).
56. Anglin, J. R., Drummond, P. & Smerzi, A. Exact quantum phase model for mesoscopic josephson junctions. *Phys. Rev. A* **64** (2001).
57. Lifshitz, E. & Pitaevskii, L. *Statistical Physics: Theory of the Condensed State (Course of Theoretical Physics, vol.9)* (Butterworth-Heinemann, 1980).
58. Kirkpatrick, S. & Gelatt, C. Optimization by simulated annealing. *Science* **220**, 671 (1983).
59. Aardal, K., Nemhauser, G. & Weismantel, R. (Eds). *Handbook of Discrete Optimization* (Elsevier, 2005).
60. Dickson, N. *et al.* Thermally assisted quantum annealing of a 16-qubit problem. *Nature Comms* **4**, 1903 (2013).
61. Kohler, S. & Sols, F. Oscillatory decay of a two-component bose-einstein condensate. *Phys. Rev. Letts* **89** (2002).
62. Sedov, E. S., Alodjants, A. P., Arakelian, S. M., Lin, Y. Y. & Lee, R.-K. Nonlinear properties and stabilities of polaritonic crystals beyond the low-excitation-density limit. *Phys. Rev. A* **84** (2011).
63. Chestnov, I., Demirchyan, S., Alodjants, A., Rubo, Y. & Kavokin, A. Permanent rabi oscillations in coupled exciton-photon systems with pt-symmetry. *Scientific Reports* **6** (2016).
64. Johnson, M. *et al.* Quantum annealing with manufactured spins. *Nature* **473** (2011).

Acknowledgements

We acknowledge the financial support from RFBR, Grants No. 15-52-52001 and No. 15-59-30406. A. Kavokin acknowledges the support from HORIZON 2020 RISE project CoExAn (Grant No. 644076) and the EPSRC Established Career fellowship on Quantum Polaritonics RP 008833. T. Lu acknowledges the support from Minister of Science and Technology (MOST) under Contract Nos MOST 104-2923-E-009-003-MY3.

Author Contributions

A.P.A. and A.V.K. proposed the idea. A.P.A., M.E.L. and D.A.D. have developed the idea and the formalism. M.E.L. and K.B.H. performed all calculations. A.P.A. and T.C.L. contributed to discussions. A.P.A., A.V.K. and T.C.L. have written the paper. All authors reviewed the manuscript.

Additional Information

Supplementary information accompanies this paper at doi:[10.1038/s41598-017-09824-8](https://doi.org/10.1038/s41598-017-09824-8)

Competing Interests: The authors declare that they have no competing interests.

Publisher's note: Springer Nature remains neutral with regard to jurisdictional claims in published maps and institutional affiliations.



Open Access This article is licensed under a Creative Commons Attribution 4.0 International License, which permits use, sharing, adaptation, distribution and reproduction in any medium or format, as long as you give appropriate credit to the original author(s) and the source, provide a link to the Creative Commons license, and indicate if changes were made. The images or other third party material in this article are included in the article's Creative Commons license, unless indicated otherwise in a credit line to the material. If material is not included in the article's Creative Commons license and your intended use is not permitted by statutory regulation or exceeds the permitted use, you will need to obtain permission directly from the copyright holder. To view a copy of this license, visit <http://creativecommons.org/licenses/by/4.0/>.

© The Author(s) 2017